Anomalous behavior of the acoustic phonon velocity and elastic constants of relaxor ferroelectric $PbMg_{1/3}Ta_{2/3}O_3$

2007 J. Phys.: Condens. Matter 19 496206

(http://iopscience.iop.org/0953-8984/19/49/496206)

IOP PUBLISHING JOURNAL OF PHYSICS: CONDENSED MATTER

J. Phys.: Condens. Matter **19** (2007) 496206 (9pp) doi:10.1088/0953-8984/19/49/496206

Anomalous behavior of the acoustic phonon velocity and elastic constants of relaxor ferroelectric $PbMg_{1/3}Ta_{2/3}O_3$

S G Lushnikov[1,5], A I Fedoseev[1], S N Gvasaliya[2,6], J-H Ko[3] and Seiji Kojima[4]

[1] Ioffe Physico-Technical Institute of Russian Academy of Sciences, 194021 St Petersburg, Politekhnicheskaya street, 26, Russia
[2] Laboratory for Neutron Scattering, ETH Zurich and Paul Scherrer Institut, CH-5232 Villigen PSI, Switzerland
[3] Department of Physics, Hallym University, 39 Hallymdaehakgil, Chuncheon, Gangwondo 200-702, Korea
[4] Institute of Materials Sciences, University of Tsukuba, Tsukuba, Ibaraki 305-8573, Japan

E-mail: sergey.lushnikov@mail.ioffe.ru

Received 25 July 2007, in final form 15 October 2007
Published 12 November 2007
Online at stacks.iop.org/JPhysCM/19/496206

Abstract

The behavior of longitudinal acoustic (LA) and transverse acoustic (TA) phonons in a cubic relaxor $PbMg_{1/3}Ta_{2/3}O_3$ (PMT) ferroelectric has been investigated by Brillouin light scattering. Analysis of the temperature dependences of phonon velocity in the temperature range from 50 to 870 K has revealed anomalies in the vicinity of the Burns temperature ($T_B \approx 570$ K) for LA phonons and a wide frequency-dependent minimum of the velocities of LA and TA phonons in the same temperature region as the dielectric response anomaly. Using experimental data, temperature dependences of the C_{11} and C_{44} elastic constants have been calculated. The elastic constants have been found to be frequency-independent in the gigahertz range. The results obtained are discussed in the framework of modern ideas on the crystalline lattice dynamics of relaxor ferroelectrics.

(Some figures in this article are in colour only in the electronic version)

1. Introduction

The relaxor state that arises in a number of disordered ferroelectric crystals has been a subject of intense investigation during the last few decades [1–4]. The interest of researchers in this

[5] Author to whom any correspondence should be addressed.
[6] On leave from: Ioffe Physico-Technical Institute of Russian Academy of Sciences, 194021 St Petersburg, Politekhnicheskaya street, 26, Russia.

state is due to the importance of the problem of the dynamics of structural phase transitions in partially disordered crystals (one of the sublattices is partially disordered) and also due the wide use of relaxor ferroelectrics in industry.

Crystals of lead magnesium tantalate $PbMg_{1/3}Ta_{2/3}O_3$ (PMT) are representatives of a large family of relaxor perovskite-like ferroelectrics with the common formula $AB'B''O_3$ [5]. Though the parent compound of relaxor ferroelectrics (from here on—relaxors) is classical ABO_3 perovskites, the relaxors exhibit properties radically differing from those of the parent compound. For instance, the dielectric response of PMT demonstrates a frequency-dependent anomaly spread for several hundred degrees with a maximum at $T_0 \approx 170$ K at 10 kHz [6]. In contrast to classical ferroelectrics, the anomalies in the dielectric response of relaxors are not directly associated with a structural phase transition. The x-ray and neutron diffraction analyses of PMT crystals have revealed the absence of a structural phase transition in the range of temperatures from 1.5 to 730 K [7–9], which is also typical of the related relaxor compound $PbMg_{1/3}Nb_{2/3}O_3$ (PMN). However, in contrast to PMN, the PMT crystals remain cubic (with $Pm\bar{3}m$ symmetry) even if an external electric field is applied [5, 9]. The absence of a structural instability makes PMT crystals suitable model objects for studying the relaxor ferroelectric state. The crystalline lattice dynamics of PMT crystals have been investigated by dielectric, optical, and neutron spectroscopy [6, 10–13] and specific heat measurements [14]. Inelastic neutron scattering experiments have revealed that characteristic features of the low-frequency region of the vibration spectrum of cubic relaxor ferroelectrics are a narrow central peak and a relaxation mode (quasi-elastic scattering—QE) [13, 15–18]. At the temperature at which the QE scattering arises, damping of the low-energy phonons starts to increase, which may be a consequence of the scattering by dynamic polar nanoregions [17, 18]. The temperature evolution of optical phonons in PMT was studied by Raman scattering in [10]. It was found that the integrated susceptibilities of the phonon peaks exhibit an anomalous behavior in the range of a strong frequency dispersion of the dielectric permittivity of PMT. In addition, the Raman line shape of the high-frequency phonon in PMT becomes more asymmetric at temperatures lower than T_0. The first results of the studies of the behavior of longitudinal acoustic phonons in PMT and their comparison with the behavior of longitudinal acoustic phonons in $PbMg_{1/3}Nb_{2/3}O_3$ and $BaMg_{1/3}Ta_{2/3}O_3$ were reported in [6]. However, to our knowledge, no thorough studies of the behavior of acoustic phonons in $PbMg_{1/3}Ta_{2/3}O_3$ have been carried out so far. For this reason, detailed investigations of the behavior of acoustic phonons in PMT crystals are of high importance.

This paper discusses the data for a PMT crystal obtained in Brillouin light scattering experiments in the temperature range from 870 to 50 K, including both the region of formation of polar nanoregions $T_B \approx 570$ K [6, 9] (which are believed to be responsible for the relaxor state [19]) and the region of the anomalous behavior of the dielectric response.

2. Experimental details

The Brillouin scattering measurements in the PMT crystal involved the use of a 3 + 3-pass Fabry–Perot interferometer (J Sandercock tandem) with an optical microscope. The source of scattered light excitation was an Ar^+-ion laser with a wavelength $\lambda_0 = 514.5$ nm. The radiation power was not higher than 100 mW. Two scattering geometries were used: 90° and 180°. In the case of a 180°-geometry, the samples were mounted in an optical cell (THMS 6000) where temperature was varied from 870 to 80 K with a stabilization of ±0.1 K. In the 90°-geometry, a furnace and an optical cryostat, where temperature variations were controlled with the same accuracy and in approximately the same temperature range with the help of a digitized temperature controller (SI9650/Lakeshore331) and a closed-cycle helium refrigerator

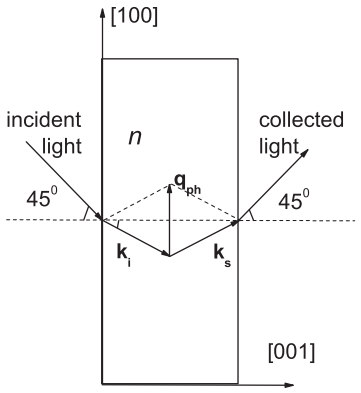

Figure 1. Scheme of the 90A geometry of the Brillouin light scattering experiment.

(RMC LTS-22), respectively, were used. Note that in the experiments described above, the same PMT crystal as in Raman light scattering and inelastic neutron scattering experiments was used [10, 12, 13]. The crystal was in the form of a parallelepiped $6.5 \times 4.5 \times 1.6$ mm^3 in size whose polished faces were oriented along the [100], [010], and [001] directions. The error in the sample orientation accomplished with an x-ray diffractometer was less than 1°.

The acoustic phonon velocity (V) in a Brillouin light scattering experiment is determined by the frequency shift ($\Delta\nu$) as

$$\begin{aligned} Vq &= \omega = 2\pi\Delta\nu, \\ q &= (4\pi n/\lambda_0)\sin(\theta/2), \end{aligned} \tag{1}$$

where q, n, and θ are the wavevector, refractive index, and the angle between the incident and scattered light, respectively. In the 180° light scattering geometry ($\theta = 180°$), acoustic phonons with wavevector $\mathbf{q}_{\rm ph} \parallel [100]$ were studied, polarizations of the incident and scattered light were oriented along [010]. Then, according to the selection rules [20], the scattering spectrum of a crystal with a cubic symmetry contains only one purely longitudinal phonon mode (LA) whose (V^a) velocity is given by

$$V^a_{\rm LA} = \frac{\lambda_0 \Delta\nu^a_{\rm LA}}{2n}. \tag{2}$$

Index a designates the 180° experimental geometry. In the 90A ($\theta = 90°$) scattering geometry the light was incident at angle 45° to the crystal face (see figure 1). In this geometry, acoustic phonons with $\mathbf{q}_{\rm ph} \parallel [100]$ and polarizations of the incident and scattered light oriented along [010] were studied. The scattering spectrum of the PMT crystal contained a purely longitudinal and a purely transverse (TA) phonon mode (figure 2(b)) whose velocities $V^b_{\rm LA}$ and $V^b_{\rm TA}$ are given by

$$V^b_{\rm LA} = \frac{\lambda_0 \Delta\nu^b_{\rm LA}}{\sqrt{2}}; \tag{3}$$

$$V^b_{\rm TA} = \frac{\lambda_0 \Delta\nu^b_{\rm TA}}{\sqrt{2}}; \tag{4}$$

where $\Delta\nu^b_{\rm LA}$ and $\Delta\nu^b_{\rm TA}$ are the frequency shifts of the longitudinal and transverse acoustic phonons (index b denotes the 90A geometry). An important advantage of the 90A light scattering geometry is that the refractive index (whose absolute value for PMT is not known) does not affect the phonon velocity being measured in such geometry [21]. The free spectral interval of the tandem was 30 or 75 GHz.

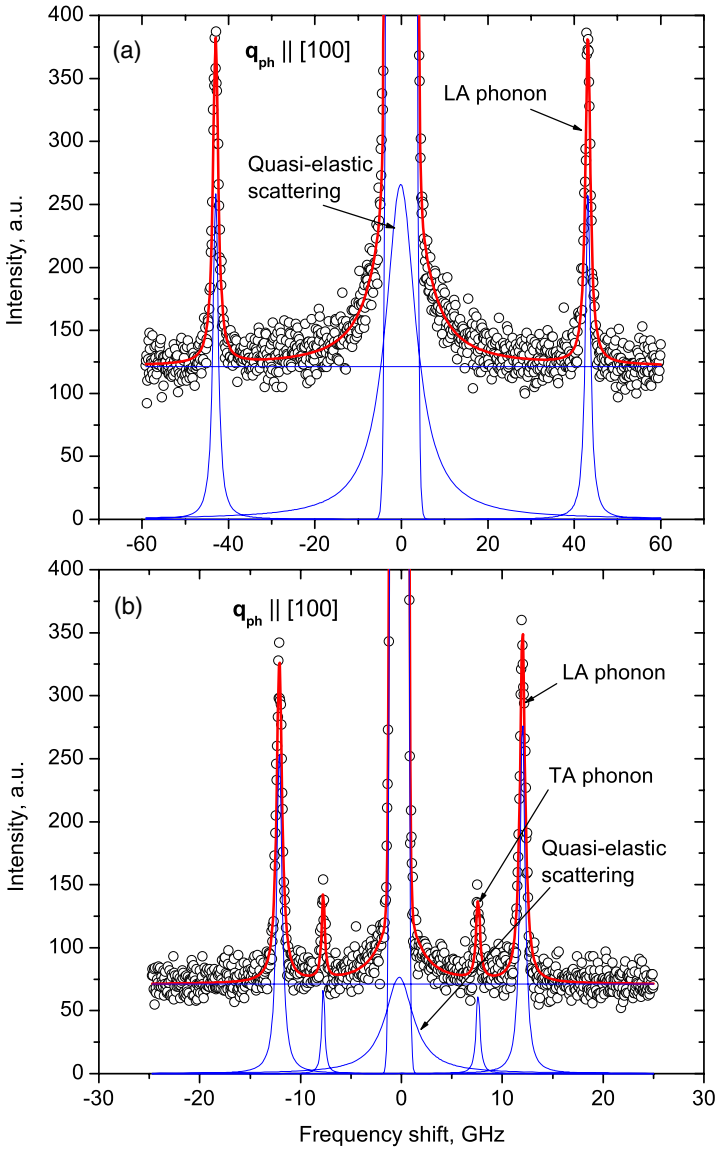

Figure 2. Experimental spectrum of the Brillouin light scattering at room temperature in the 180° scattering geometry (a) and 90A geometry of scattering (b).

3. Results and discussion

Examples of experimental spectra are shown in figure 2. The results were processed by the least squares method. The fitting functions in calculations of phonon line shapes and scattering at an unshifted frequency were the Lorentz and Gauss functions, respectively. It is clearly seen from figure 2 that there is an additional contribution at the unshifted frequency, i.e. the quasi-elastic scattering described by the Lorentz function. (The behavior of the quasi-elastic scattering with varying temperature will be discussed elsewhere.) The temperature dependences of the frequency shifts of LA and TA modes obtained by processing the spectra

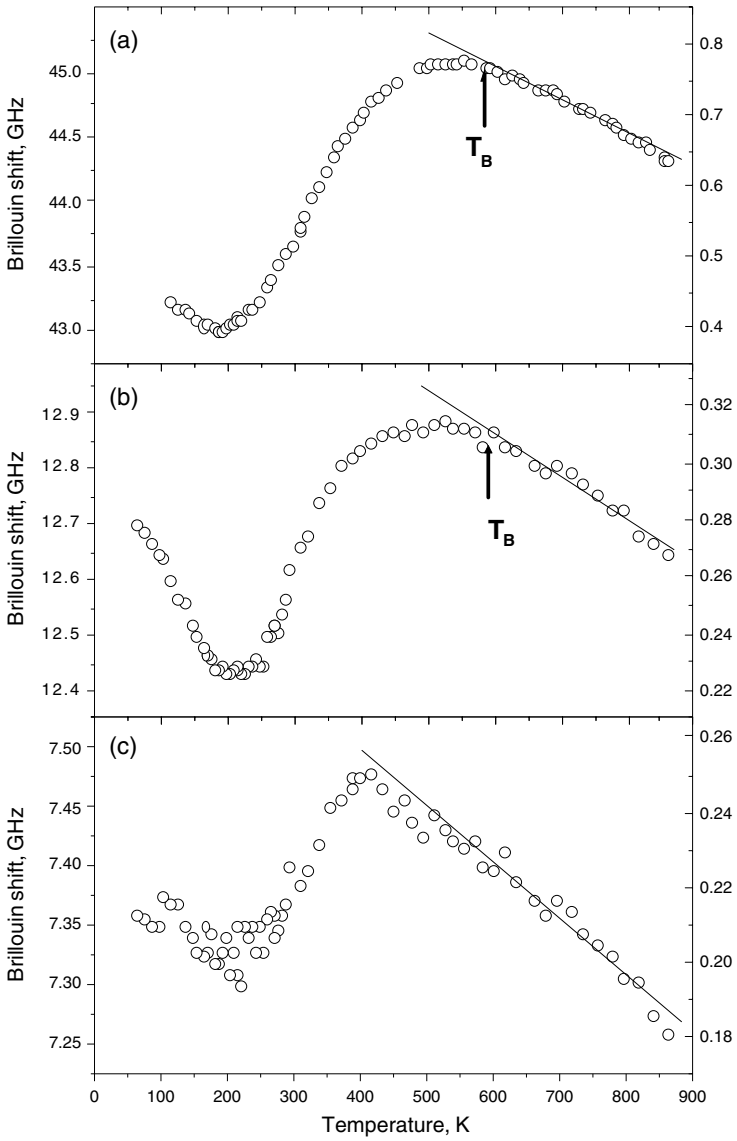

Figure 3. Temperature dependences of the Brillouin shift for (a) the LA phonon obtained in the 180° geometry of scattering and (b) LA and (c) TA phonons obtained in the 90A geometry of scattering.

are presented in figure 3. The dependences shown in figure 3 are seen to be typical of relaxors, i.e. a wide minimum of the frequency shift as a function of temperature is observed. In accordance with equations (2)–(4), the frequency shift is directly proportional to the acoustic phonon velocity, and for this reason we shall consider below the behavior of the velocity rather than of the frequency shift. In the high-temperature region, the velocity linearly depends on temperature. The deviation of the temperature dependence of the LA phonon velocity from a linear dependence is observed in the vicinity of the temperature of polar nanoregion formation ($T_B \approx 570$ K) (figures 3(a) and (b)). For the first time this phenomenon was associated with the formation of nanoregions in the analysis of Brillouin light scattering in PMN crystals [22].

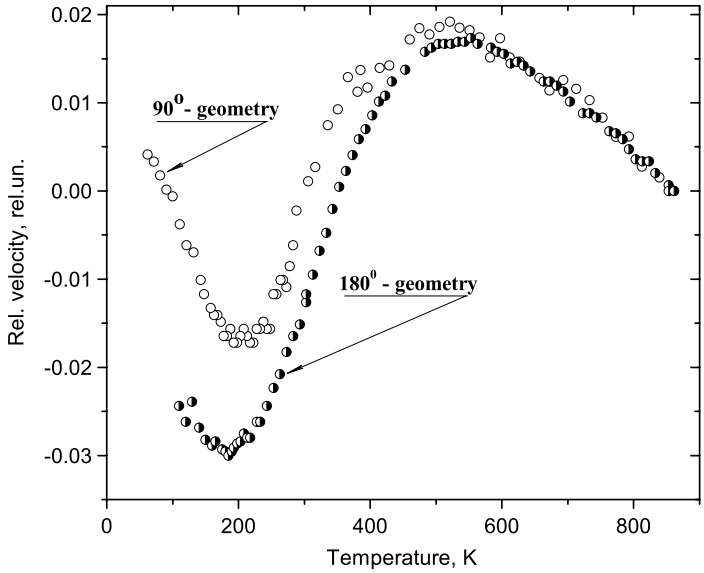

Figure 4. Temperature evolution of relative changes in the sound velocity of the LA phonon. Temperature variations of refractive index were taken into account in calculations of the sound velocity in the 180° geometry.

Later the effect of polar nanoregions on the behavior of acoustic phonons was also revealed in the relaxor compound lanthanum lead zirconate titanate [23]. The deviation of the temperature dependence of the TA phonon velocity from being linear begins at a much lower temperature, in the vicinity of 500 K (figure 3(c)). Softening of the LA phonon velocity starting in the vicinity of T_B reaches a minimum at ≈190 K and grows with decreasing temperature (see figures 3 and 4). The minima of phonon velocities correspond to the dielectric response anomaly of the PMT crystal [6]. The magnitude of variations in the LA phonon velocity is from 3.5 to 5%, depending on the measurement frequency (below we consider the frequency dependence of velocity in more detail). Thus, on the whole, the TA phonon behavior is similar to that of the LA phonons, though the velocity minimum in the temperature dependence of the TA phonon velocity is less pronounced. The magnitude of variations in the TA phonon velocity is about 2.5%. It is interesting to note that the behavior of the phonon velocity in PMT is similar to that in disordered crystals at phase transition into a glass-like state [24]. It is known that a characteristic feature of the transition into a glass-like phase is a strong frequency dependence of the acoustic response. This necessitated analysis of the frequency dependence of the LA phonon velocity in the PMT crystal.

Note that one can determine the elastic constant C_{11} from the velocities of the LA phonons studied in different geometries. Changes in the angle of scattering in different experimental geometries vary the wavevector of the LA phonon and, hence, the probe frequency according to equation (1). This allows analysis of the LA phonon behavior at frequencies $f \approx 45$ and 13 GHz (180° and 90A scattering geometries, respectively) in a wide temperature range. To analyze the results, we plot relative variations in the frequency shift $\delta\nu_{LA} = (\Delta\nu(T) - \Delta\nu_0)/\Delta\nu_0$ measured in different experimental geometries, where $\Delta\nu_0$ is taken to be the magnitude of the frequency shift at $T = 690$ K. It can be seen from figure 4 that the temperature at which the velocity has a minimum depends on frequency; for the phonons with a probe frequency of 45 GHz the minimum is observed in the vicinity

Table 1. Elastic constants of PMT and PMN crystals.

	PMT			PMN[c]		
T (K)	C_{11}^E (GPa)[a]	C_{11}^E (GPa)[b]	C_{44}^E (GPa)	C_{11}^E (GPa)[a]	C_{11}^E (GPa)[b]	C_{44}^E (GPa)
800	206.11	206.91	68.196	179.08	174.16	71.018
700	209.25	209.55	69.414	180.67	176.27	72.193
600	211.67	211.52	69.924	180.11	175.86	72.211
500	212.65	212.04	70.796	177.02	173.28	72.071
400	209.87	209.19	71.105	169.53	166.13	71.877
300	202.49	204.83	69.678	162.78	155.45	68.387
200	197.57	198.03	68.270	164.65	157.40	68.096
100		202.83	69.396	170.22	161.46	69.471

[a] C_{11}^E—the magnitude of the elastic constant is obtained in the experiments with the 180° scattering geometry, $\mathbf{q}_{\rm ph} \parallel [100]$.
[b] C_{11}^E—the magnitude of the elastic constant is measured in the experiments with the 90A scattering geometry, $\mathbf{q}_{\rm ph} \parallel [100]$.
[c] Data are taken from [29].

of 170 K, and for a frequency of 13 GHz a minimum is observed around 210 K. Thus, the velocity minimum shifts towards higher temperatures as the frequency of measurements decreases. The dispersion in the behavior of the LA phonon velocity in PMT in this frequency range is not typical of the frequency dependence of acoustic anomalies in the vicinity of structural phase transitions. For instance, at a ferroelectric phase transition in TGS crystals, a decrease in the probe frequency leads to a shift of acoustic anomalies to a low-temperature region (a ferroelectric phase) [25]. The acoustic response in $AgNa(NO_2)_2$ crystals behaves similarly [26]. The acoustic response dispersion in the vicinity of structural phase transitions can be explained in the framework of relaxation mechanisms. In the case of the PMT and PMN relaxor ferroelectrics, a decrease in frequency leads to a shift of the velocity minimum to the high-temperature region (a paraphase), which is opposite to the velocity behavior at structural phase transitions. Thus, it can be concluded that the classical relaxation mechanism is not a determining factor in the velocity dispersion in the gigahertz region in PMN and PMT crystals. To find the mechanism responsible for velocity dispersion, additional investigations of the acoustic response of relaxors in a wide frequency range are required.

The results obtained in the Brillouin light scattering experiments allowed us to calculate elastic constants C_{11} and C_{44} (equations (5)–(7)) and plot their temperature dependences (figure 5).

$$\rho(V_{\rm LA}^a)^2 = C_{11}^a \tag{5}$$

$$\rho(V_{\rm LA}^b)^2 = C_{11}^b \tag{6}$$

$$\rho(V_{\rm TA}^b)^2 = C_{44}^b, \tag{7}$$

where $\rho = 9.65\ \mathrm{g\,cm^{-3}}$ [27]. Using the data for the LA phonon obtained in the 180° and 90A scattering geometries and equations (2) and (3) we calculated the refractive index n at $T = 693$ K under the assumption that the hypersound velocity dispersion is absent above the Burns temperature

$$n = \frac{\Delta\nu_{11}^a}{\Delta\nu_{11}^b\sqrt{2}} = \frac{44.83}{12.807 \times \sqrt{2}} \approx 2.475. \tag{8}$$

Then, using the data on the temperature behavior of relative variations in the refractive index given in [28], a temperature behavior of elastic constant C_{11}^a was calculated from equation (1). Table 1 gives elastic constants C_{11} and C_{44} obtained for PMN and PMT crystals in the Brillouin

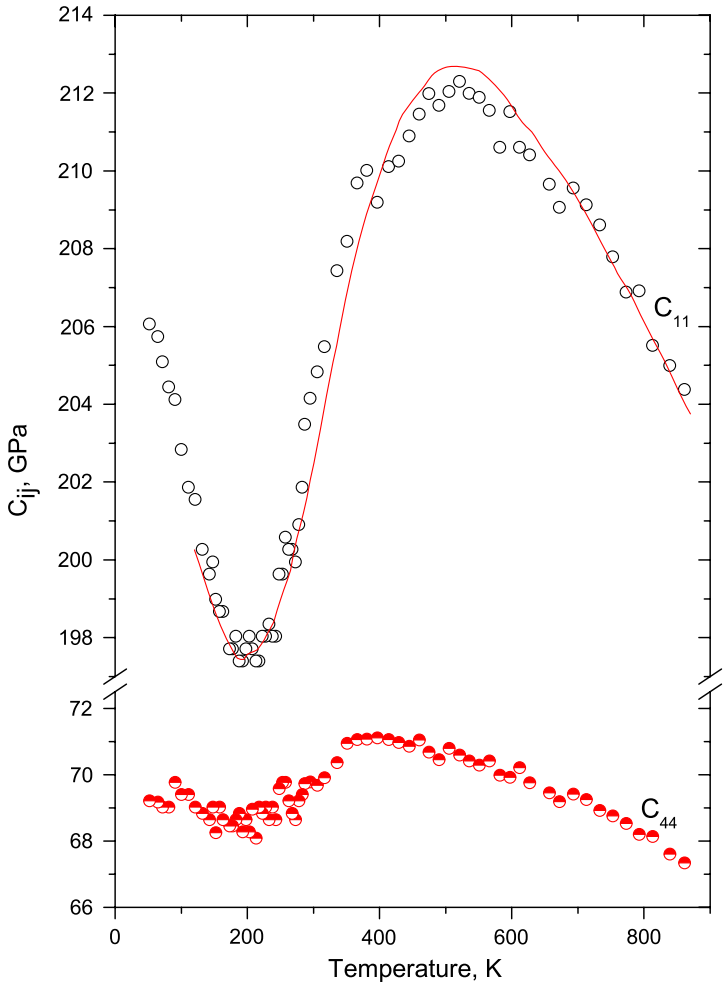

Figure 5. Temperature dependences of C_{11} and C_{44} elastic constants. The solid line is a result of calculations of the C_{11} elastic constant from the data obtained in the 180° scattering geometry (see the text).

light scattering experiments performed under similar conditions, i.e. in the 180° and 90A geometries. Comparative analysis has shown that the magnitudes of C_{11} for PMT are higher than for PMN in the entire range of the temperatures studied. The values of C_{44} are similar for both crystals in the low-temperature region and differ remarkably in the high-temperature region. Comparison of the temperature evolutions of elastic constant C_{11} in the PMT crystal at different frequencies (figure 5) has revealed that there is no dispersion of C_{11} in the gigahertz range (within the limits of measuring error and under the condition of absence of the velocity dispersion above T_B). A radically different behavior is exhibited by C_{11} in the PMN crystal: a strong dispersion of C_{11} was observed in the vicinity of the dielectric response anomaly [29].

4. Conclusions

To summarize, as evidenced by Brillouin light scattering experiments, the formation of polar nanoregions in the PMT crystal leads to changes in the behavior of longitudinal acoustic

phonons. A wide anomaly in the velocity of acoustic phonons has been found to correspond to the anomaly in the dielectric response of PMT. The dispersion of the velocity of longitudinal acoustic phonons, which cannot be explained by the classical relaxation mechanism, has been observed. The refractive index of PMT has been determined. The magnitudes of the C_{11} and C_{44} elastic constants of PMT have been calculated, and their temperature dependences have been plotted.

Acknowledgments

The work was supported by the grants of the President of the Russian Federation (SS-1415.2003.2), Russian Foundation for Basic Research 05-02-17583. One of the authors (SGL) is grateful to the Japan Society for the Promotion of Science Invitation Fellowship Program for Research in Japan, and to the Institute of Materials Science, University of Tsukuba, for its hospitality.

References

[1] Grinberg I, Cooper V R and Rappe A M 2002 *Nature* **419** 909
[2] Kutnjak Z, Petzelt J and Blinc R 2006 *Nature* **441** 956
[3] Fu H and Cohen R E 2000 *Nature* **403** 283
[4] Xu G, Zhong Z, Ye Z-G and Shirane G 2006 *Nat. Mater.* **5** 134
[5] Smolenskii G A *et al* 1984 *Ferroelectrics and Related Materials* (London: Gordon and Breach)
[6] Ko J-H, Kojima S and Lushnikov S G 2003 *Appl. Phys. Lett.* **82** 4128
[7] Lu Z G, Flicoteaux C and Calvarin G 1996 *Mater. Res. Bull.* **31** 445
[8] Akbas M A and Davies P K 1997 *J. Am. Ceram. Soc.* **80** 2933
[9] Gvasaliya S N, Roessli B, Sheptyakov D, Lushnikov S G and Shaplygina T A 2004 *Eur. Phys. J.* B **40** 235
[10] Lushnikov S G, Gvasaliya S N and Katiyar R 2004 *Phys. Rev.* B **70** 172101
Gvasaliya S N, Lushnikov S G, Roessli B and Katiyar R 2004 *Ferroelectrics* **302** 593
[11] Gvasaliya S N, Lushnikov S G, Sashin I L and Shaplygina T A 2003 *J. Appl. Phys.* **94** 1130
[12] Gvasaliya S N, Roessli B and Lushnikov S G 2003 *Europhys. Lett.* **63** 303
[13] Gvasaliya S N, Lushnikov S G and Roessli B 2004 *Crystallogr. Rep.* **49** 108
[14] Moriya Y, Kawaji H, Tojo T and Atake T 2003 *Phys. Rev. Lett.* **90** 205901
[15] Gvasaliya S N, Lushnikov S G and Roessli B 2004 *Phys. Rev.* B **69** 092105
[16] Stock C, Birgeneau R J, Wakimoto S, Gardner J S, Chen W, Ye Z-G and Shirane G 2004 *Phys. Rev.* B **69** 094104
[17] Gvasaliya S N, Roessli B, Cowley R A, Huber P and Lushnikov S G 2005 *J. Phys.: Condens. Matter* **17** 4343
[18] Gvasaliya S N, Roessli B, Cowley R A, Kojima S and Lushnikov S G 2007 *J. Phys.: Condens. Matter* **19** 016219
[19] Burns G and Dacol F 1983 *Solid State Commun.* **48** 853
[20] Vacher R and Boyer L 1972 *Phys. Rev.* B **6** 639
[21] Vaughan J M 1989 *The Fabry–Perot Interferometer* (Bristol: Hilger)
[22] Prokhorova S D and Lushnikov S G 1989 *Ferroelectrics* **90** 187
[23] Shabbir G, Ko J-H, Kojima S and Yin O-R 2003 *Appl. Phys. Lett.* **82** 4696
[24] Höchli U T, Knorr K and Loidl A 1990 *Adv. Phys.* **39** 405
[25] Yagi T, Tokunaga M and Tatsuzaki I 1976 *J. Phys. Soc. Japan* **40** 1659
[26] Soprunyuk V P *et al* 2002 *Phys. Rev.* B **66** 104102
[27] Bokov V A and Myl'nikova I E 1961 *Fiz. Tverd. Tela (Leningrad)* **3** 841
Bokov V A and Myl'nikova I E 1961 *Sov. Phys.—Solid State* **3** 613 (Engl. Transl.)
[28] Korshunov O Yu, Markovin P A and Pisarev R V 1992 *Ferroelectrics* **13** 137
[29] Lushnikov S G, Fedoseev A I, Gvasaliya S N and Kojima S 2007 unpublished